Landmine Classification Using Possibilistic K-Nearest Neighbors with Wideband Electromagnetic Induction Data

J. Dula[a], A. Zare[a], D. Ho[a], P. Gader[b]
[a]University of Missouri, Columbia, MO 65211 [b]University of Florida, Gainesville, FL 32611

ABSTRACT

A possibilistic K-Nearest Neighbors classifier is presented to classify mine and non-mine objects using data collected from a wideband electromagnetic induction (WEMI) sensor. The proposed classifier is motivated by the observation that buried objects often have consistent signatures depending on their metal content, size, shape, and depth. Given a joint orthogonal matching pursuits (JOMP) sparse representation, particular target types consistently selected the same dictionary elements. The proposed classifier distinguishes between target types using the frequency of dictionary elements selected by potential landmine alarms. Results are shown on data containing sixteen landmine types and several non-mine examples.

Keywords: Possibilistic K-nearest neighbors, Joint Orthogonal Matching Pursuits, Dictionary Elements, Wide-band Electromagnetic Induction, Landmine, Detection, Target Classification

1. INTRODUCTION

In this paper, an algorithm for landmine classification using wide-band electromagnetic induction (WEMI) [1] data is presented. A number of algorithms in the literature have been developed for landmine detection using EMI data [2][3][4][5][6][7][9][10][14]. The algorithm proposed here classifies data points using a possibilistic K-nearest neighbors (K-NN) classifier [13] given features extracted using a Joint Orthogonal Matching Pursuits (JOMP) procedure [15]. In the following, an overview of the JOMP algorithm used to extract features is described. Section 3 discusses the proposed extensions to the possibilistic K-NN classifier such that this method can be applied to WEMI data using JOMP features and presents the proposed algorithm, the WEMI Possibilistic K-Nearest Neighbors Algorithm, WPK-NN. In Section 4, results on data containing sixteen landmine types and several non-mine examples are presented. Finally, Section 5 includes a summary and discussion of future work.

2. JOINT ORTHOGONAL MATCHING PURSUITS

In this work, the Joint Orthogonal Matching Pursuits [15] algorithm (JOMP) is used to extract features that will be used within the WPK-NN classifier. JOMP is an extension of the orthogonal matching pursuits (OMP) approach for sparse signal representation [8]. In OMP, a signal, x_j, is represented with dictionary elements, $D = \{d_i\}_{i=1}^{M}$, using a sparse, linear combination, $x_j = \sum_{k=1}^{m} w_{kj} d_k$ where $m<<M$. OMP selects dictionary elements to represent a data point using an iterative greedy approach. JOMP extends OMP by considering multiple signals simultaneously and uses the same sequence of dictionary elements to represent all of these signals [15]. In our implementation, JOMP is used to estimate a sparse representation of multiple data points symmetrically placed around a central point of interest as shown in Figure 1. Figure 1 shows the central point x_i for which JOMP confidence is assigned by looking at two points $r_1 = x_i - q$ and $r_2 = x_i + q$.

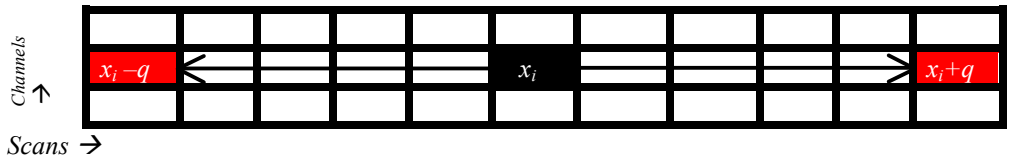

Figure 1: JOMP confidence assignment given two responses analyzed jointly

For the proposed classifier, the following features are extracted using the JOMP algorithm: (1) the dictionary elements selected by JOMP for set of points over a potential target location and (2) a confidence value assigned based on the residual errors of the points being considered,

Detection and Sensing of Mines, Explosive Objects, and Obscured Targets XVIII, edited by J. Thomas Broach, Jason C. Isaacs, Proc. of SPIE Vol. 8709, 87091F · © 2013 SPIE
CCC code: 0277-786X/13/$18 · doi: 10.1117/12.2016490

$$c_x = \frac{1}{1 + \frac{1}{n}\sum_j r_j} \quad (1)$$

where r_j is the residual error for the j^{th} point being considered simultaneously. This confidence provides a measure of how well the dictionary can represent the points under consideration. Three sets of dictionary elements are considered for the WEMI data as described in Section 3.

3. POSSIBILISTIC K-NEAREST NEIGHBOR CLASSIFIER FOR WEMI DATA

The standard K-nearest neighbor (K-NN) classifier classifies a test point using a voting scheme based on the *K*-closest labeled training examples [11][12]. Extensions to this include the Fuzzy K-NN classifier in which neighbors are weighted based on their relative distance to the test point and each training point's membership degree in the class [12]. However, these K-NN classifiers do not make use of the absolute distance between input test points and training examples. Thus, these methods are not able to distinguish between test points that are close (i.e. points that are typical of the data set) or vary far (i.e. outliers) from their K-nearest training examples. Instead, these approaches rely only on the relative distance between a test point and the K-nearest training examples used for classification. Thus, the K-NN and fuzzy K-NN classifiers will classify outliers with as much confidence as test points that are very typical of a data set. This drawback was addressed with possibilistic K-NN classifiers in which classification confidence takes into account the absolute distance between a test point and its K-nearest training samples. For example, [13] presented a possibilistic K-NN classifier for landmine detection using ground-penetrating radar data.

In WEMI data, signatures of buried objects are dependent on their metal content, size, shape, depth and material properties. Therefore, objects of a particular type often have similar signatures and select consistent dictionary elements in the JOMP algorithm. To illustrate this, consider Figure 2 in which the frequency responses from three target types are presented with their Argand diagrams. An Argand diagram is a plot of the real versus imaginary components of the frequency response across a range of frequency values. Each row of Figure 2 shows the frequency response over three objects of the same target type. As can be seen, the shape of these responses are consistent. In the proposed approach, this fact is used in order to discriminate different target types.

In the proposed possibilistic K-NN classifier, a confidence is assigned for each test point into one of *R* classes. This confidence is assigned based the distance between test points and the dictionary elements used in the JOMP sparse representation. The possibilistic classifier is used in two stages: training and testing.

3.1. Training

Training data for the proposed method is comprised of alarm locations along with their true classification labels. Each alarm location consists of a set of frequency response signatures over the potential target object. The JOMP algorithm was applied over each response in the alarm location and the dictionary index chosen along with its JOMP confidence was computed. This gives a dictionary index map, which indicates the dictionary index chosen by every point in each training alarm. We use this dictionary index map in order to get the overall dictionary counts of each target type associated with each dictionary element for the training data set. In order to account for bias based on the number of alarms in the training set per target type, these counts are normalized. The normalized dictionary counts, D, are found by computing $n_{rj,}$ the number of pixel locations from the r^{th} target type represented with j^{th} dictionary element in the training data, and normalizing across dictionary elements,

$$d_{rj} = \frac{n_{rj}}{\sum_k n_{rk}} \quad (2)$$

Let this matrix be represented by D,

$$D = \begin{bmatrix} d_{11} & \cdots & d_{1k} \\ \vdots & \ddots & \vdots \\ d_{r1} & \cdots & d_{rk} \end{bmatrix} \quad (3)$$

These dictionary counts are used in the proposed classifier to weight dictionary element selections by a test point using the number of training points of each target type represented by that dictionary element.

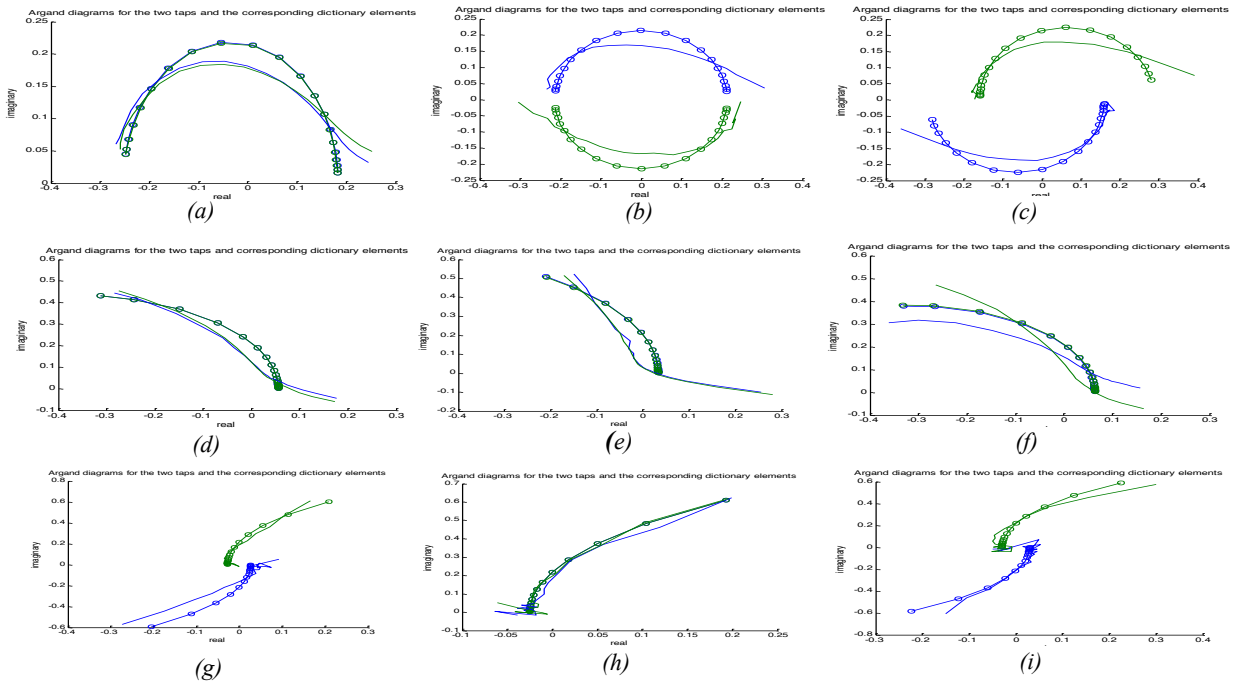

Figure 2: (a)-(c) Argrand diagrams for the two taps and the corresponding dictionary element for target type I (d)-(f) Argrand diagrams for the two taps and the corresponding dictionary element for target type II (g)-(i) Argrand diagrams for the two taps and the corresponding dictionary element for target type III

3.2. Testing

For each test alarm, a_i, the JOMP algorithm is applied to each frequency response in the alarm. Then, the K most frequently selected dictionary elements for the test alarm are identified. Also, the residual error of every point in the alarm blob is calculated when projected on those K dictionary elements. The residual error is used as a distance measure between the dictionary element and each pixel in the alarm. The mean of these residuals errors are then averaged and used, in conjunction with the normalized dictionary counts learned in training, to assign a confidence value for the alarm in each target type. Each of the K neighbors are assigned a possibilistic weight as shown below,

$$W_{ik} = \frac{1}{1 + \left[max\left(0, \left(\frac{R_{ik} - \eta_1}{\eta_2}\right)\right)\right]^{\frac{2}{m-1}}} \qquad (4)$$

where W_{ik} is the possibilistic weight of the alarm to the k^{th} neighbor, R_{ik} = mean residual of the alarm a_i to the k^{th} dictionary element, η_1, η_2 and m are parameter values. In the current implementation, η_1 is set to mean of all the residuals, η_2 set to three times the standard deviation of the residuals and m is a fuzziness parameter. In the current implementation, this parameter is set to 2. After computing W_{ik} for each class and the given test point, the confidence assignment for an alarm in a particular class is as follows,

$$P_r(a_i) = \frac{1}{K}\sum_{k=1}^{K} d_{rk} W_{ik} \qquad (5)$$

where $P_r(a_i)$ is the possibilistic confidence of the i^{th} alarm in the r^{th} target class.

Three different dictionaries were considered for the WEMI data. These include one dictionary based on the Discrete Spectrum of Relaxation Frequencies (DSRF) model and two dictionaries that were estimated from the training data. These three dictionaries are described in the following sub-sections.

3.3. Parametric DSRF Dictionary

The first set of dictionary elements considered are generated using the Discrete Spectrum of Relaxation Frequencies (DSRF) model[1] [14]. The DSRF model, shown in equation *(6)*, is used to produce dictionary elements by varying a large set of possible relaxation frequencies ζ, and using fixed values of ω that correspond to the frequencies measured by the EMI sensor. This dictionary has been shown to be to characterize materials in an EMI response [14].

$$H(\omega) = c_0 + \sum_{k=1}^{K} \frac{c_k}{1 + \frac{j\omega}{\zeta_k}} \tag{6}$$

where j = (-1). To relate the DSRF model to the MP framework, each dictionary element will correspond to a vector d_i as shown below,

$$d_i = \left[\frac{1}{1 + \frac{j\omega_1}{\zeta_i}}, \frac{1}{1 + \frac{j\omega_2}{\zeta_i}} \cdots \frac{1}{1 + \frac{j\omega_N}{\zeta_i}} \right]^T \tag{7}$$

In addition to the dictionary elements described above, a background dictionary element is generated using the following soil model,

$$R_m(\omega) = p_1 + p_2 \left[ln\left(\frac{\omega}{\omega_0}\right) + j\frac{\pi}{2} \right] \tag{8}$$

The figure below shows the DSRF dictionary generated using the model in equation *(6)*. The horizontal blue line, shows the soil response as modeled by equation (8).

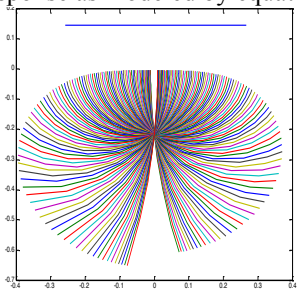

Figure 3: DSRF Dictionary along with the horizontal (blue line) soil model

3.4. Dictionary Estimated from K-Means Clustering

In addition to the DSRF dictionary, a dictionary estimated from the training data using K-Means clustering was considered. To estimate the dictionary using *K*-means clustering, the training data was divided according to the class types. Then, a simple *K*-means clustering algorithm was applied to the set of frequency responses associated with each class type. The dictionary obtained was then used to perform the JOMP algorithm and dictionary maps for each alarm were created. Using the dictionary maps, counts of the dictionary indices chosen were determined which were used as features for training the classifier. In our implementation, the number of clusters was varied from 30 to 60. In the experiments shown here, 60 clusters per target type were used. Figure 4 shows a signal and its reconstruction using all the dictionary prototypes obtained from K- means.

3.5. DICTIONARY ESTIMATED FROM LINEAR COMBINATION MODEL

A dictionary was also generated by estimating elements that minimize the error using the linear combination model from the JOMP algorithm. This is done by performing a least squares minimization of the residual sum of squares (RSS) objective function shown below,

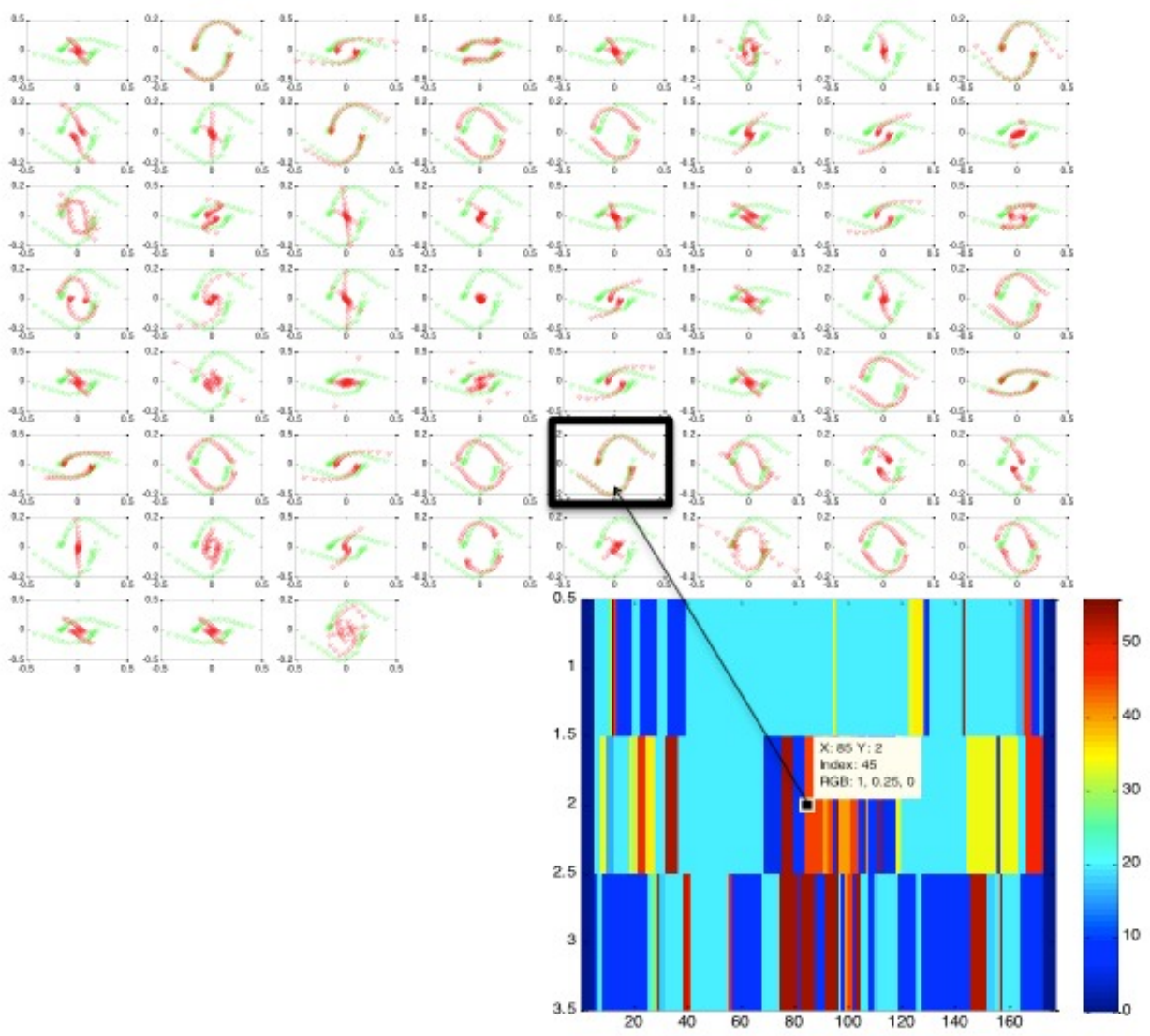

Figure 4: Dictionary map (Target Type 1) and reconstruction of one response with all estimated cluster prototypes

$$RSS_{dict} = \sum_{i=1}^{N} (x_i - c_i d)^T (x_i - c_i d) \qquad (9)$$

where c_i is weight of the dictionary element for i^{th} training point and d is the dictionary element to be estimated. In our implementation, we estimate one dictionary element per target type. This minimization is accomplished using alternating optimization. Thus, given initial dictionary values, the weights for each training point are estimated. In our implementation, dictionary estimates are determined using K-means. Then the weights are updated using $c_i = \{d^T d\}^{-1} d^T x$ followed by the dictionary element update $d = \{c^T c\}^{-1} c^T \boldsymbol{X}$. This iterative procedure is continued until the value of RSS_{dict} is smaller than a tolerance value.

4. EXPERIMENTS AND RESULTS

4.1. Data Set Description

For all the experiments, WEMI data obtained from wideband electromagnetic induction sensors were used. The sensor used measures the responses at 21 frequencies that are approximately logarithmically distributed over the

frequency range of 300 Hz-90 kHz [14]. The dataset used for testing contained 16 target types which included metal clutter. For each type of target, the WEMI response is collected from several targets buried at different depths and location. A distribution of the target types is shown in Table 1. This table includes a classification based on metal content into non-metal, low-metal and high-metal. The purpose field classifies the targets as either anti-tank (AT) or anti-personal (AP). Each of these targets is encountered multiple times in the dataset and hence the unique encounters are also noted in the table along with the alarms that were generated using a JOMP pre-screener when run over this full data set.

Name	Content	Purpose	Number of JOMP Alarms	Unique Encounters
Target Type 1	Low	AP	13	8
Target Type 2	Low	AP	20	8
Target Type 3	Low	AT	0	8
Target Type 4	Low	AT	2	7
Target Type 5	Low	AT	0	8
Target Type 6	Non	AT	0	8
Target Type 7	Non	AT	2	8
Target Type 8	Metal	AT	26	3
Target Type 9	Low	AT	35	8
Target Type 10	Low	AT	30	11
Target Type 11	Non	AT	0	11
Target Type 12	Non	AT	0	8
Target Type 13	Metal	AT	0	1
Target Type 14	Metal	AT	7	3
Target Type 15	Metal	AT	0	1
Target Type 16	Metal	AT	1	3
Total			**392**	**104**

Table 1: Target Distribution in WEMI data

4.2. Dictionary counts on WEMI Data

The training stage of the proposed algorithm is comprised of obtaining the counts of the dictionary elements chosen per target type. The total counts for the data set used are shown in Figure 5 and the corresponding normalized values are shown in Figure 6. These counts show the consistency in selecting dictionary elements by targets. This consistency illustrates the motivation behind using this classifier.

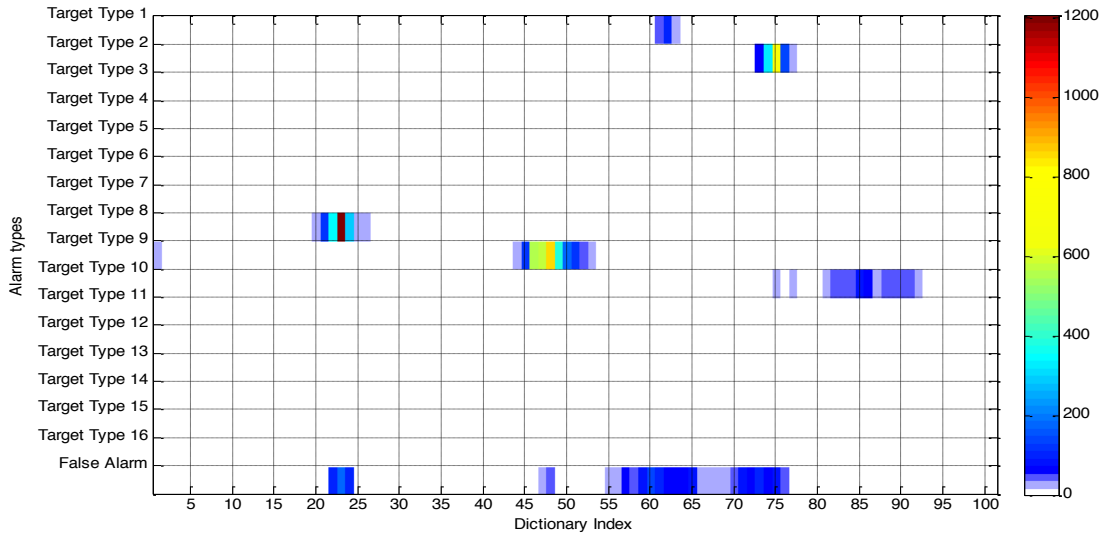

Figure 5: Dictionary counts for different target types

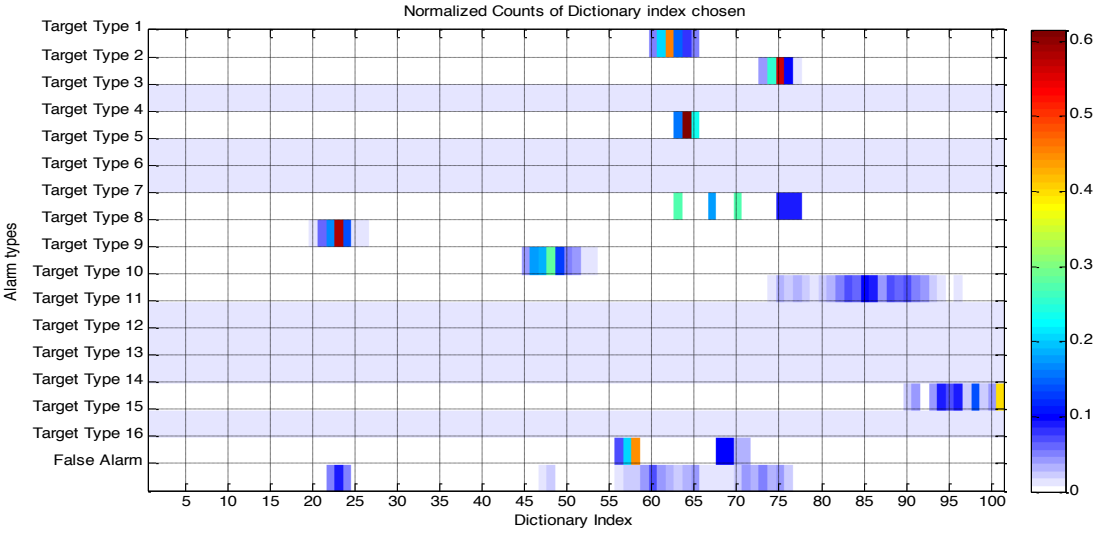

Figure 6: Normalized Dictionary counts

The dictionary maps and the corresponding Argand diagrams shown below for certain target types also show that the blob around a target chooses dictionary elements consistently. These maps further validate the use of dictionary counts as a good feature for discriminating the target types

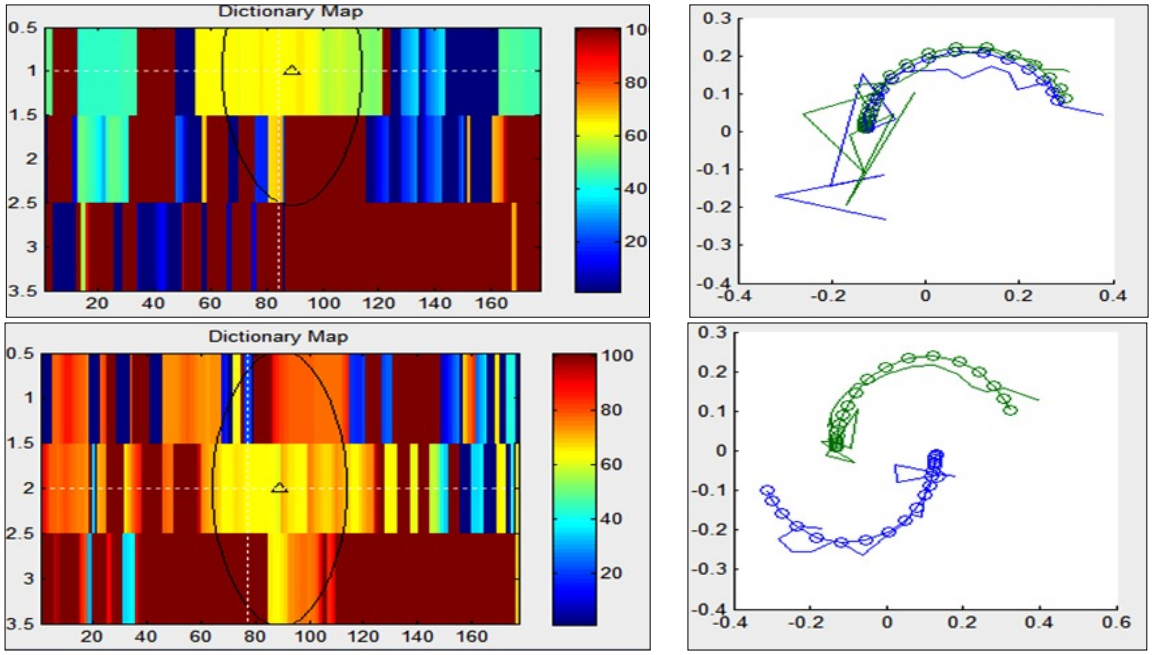

Figure 7: The dictionary maps and corresponding Argand diagrams for target type 5

4.3. DSRF Dictionary

In order to validate our results, we ran the classifier on the WEMI dataset described above. The proposed method was applied to alarms generated using the JOMP algorithm on the WEMI data. To report and compare results a Receiver Operating Characteristics Curve (ROC) is used to plot the false positives (x – axis) versus the true positives (y – axis). The x-axis shows the false alarm rate (FAR) and the y-axis shows the percentage of detection (PD). In order to generate the ROC curve, the classifier results across target type were combined into a confidence of mine vs. non-mine. The mine confidence used to generate the ROC curve was computed using

$$F(a_i) = \sum_{r \epsilon M} P_r(a_i) J(a_i) \qquad (10)$$

where $F(a_i)$ is final confidence value for test alarm, M is group of mine types and $J(a_i)$ are the confidences assigned to the test alarm during the prescreening stage to each test object.

In Figure 8, the blue curve shows the JOMP algorithm performance and the red curve shows the classifier performance in which the methods were tested on the training data using the DSRF dictionary. As can be seen from the ROCs, our method shows a significant improvement in the classifier performance at the smaller false alarm rates as opposed to JOMP which classifies some of the false alarms as mines, giving them a very high confidence. Figure 9 shows the comparison results when applied in a ten-fold cross-validation setting and using the DSRF dictionary.

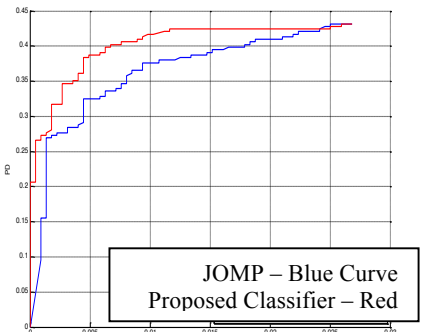

Figure 8: ROC obtained using the proposed method for the test dataset. The blue curve shows the JOMP pre-screener ROC and the red curve shows the proposed classifier results.

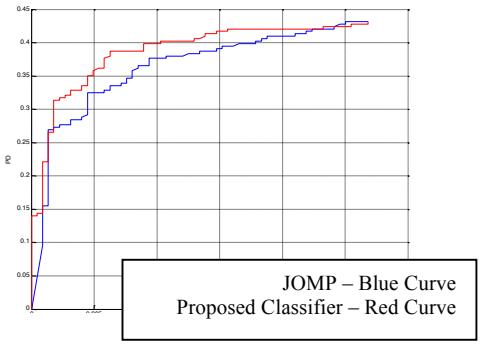

Figure 9: ROC for 10-fold cross-validation and DSRF Dictionary

4.3.1. Confusion matrix between 17 target types

The confusion matrix in Figure 10 shows the actual labels on the *y*-axis and the indicated value on the *x*-axis. For a total of 237 targets, the accuracy of classification is 64.14% within the 17 types using 10-fold cross validation. This confusion matrix is created by selecting the class that gets the maximum possibilistic weight as the indicated mine class. This confusion matrix is colored such that the blue shades represent low values and red shades show higher values. The confusion matrix shows dark shades of red along the diagonal meaning most alarms were classified as belonging to the correct class. The other parts of the matrix above and below the diagonal show lighter shades of blue meaning fewer alarms were misclassified. A weighted version of the confusion matrix is shown in Figure 10 which sums the possibilistic weights assigned to each target type. The weighted confusion matrix has a smaller possibilistic weight assigned to the false alarms classified as target type one. This shows that even though many false alarms were classified to be targets of type 1, they had lower weights. The diagonal elements have much higher weights showing more confidence in the classification.

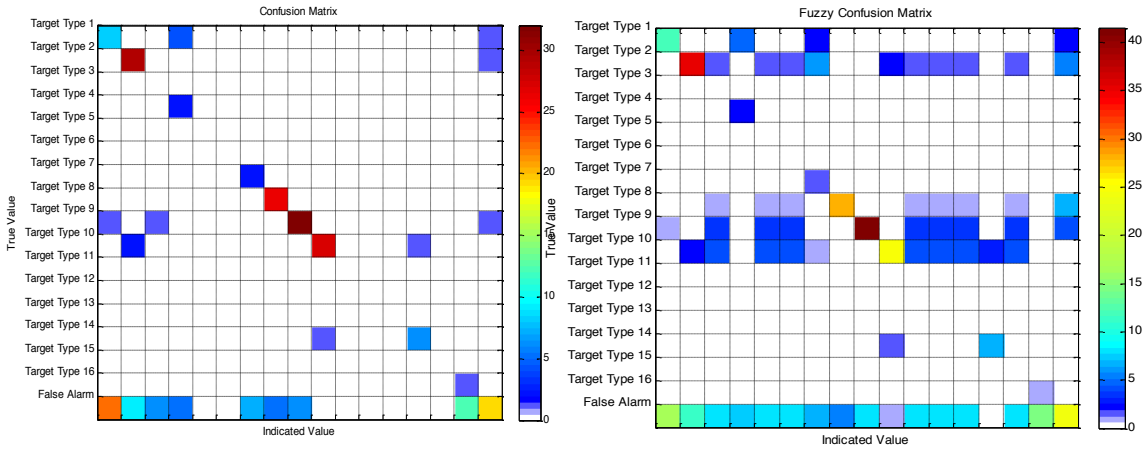

Figure 10: Confusion Matrix showing classification results among 17 target type. (b) Weighted confusion matrix showing the sum of the possibilistic weights

4.4. Dictionary Estimated using K-Means Clustering

To get an idea of the number of clusters, the K-means algorithm was run with different values of *K*. As the number of clusters was increased, more dictionary elements generated had very similar shape. In order to measure the sensitivity of the classifier to the number of clusters, the classifier was run using dictionary with number of dictionary elements ranging from 30, 35, 40, …, 60. The results obtained are shown in Figure 11.

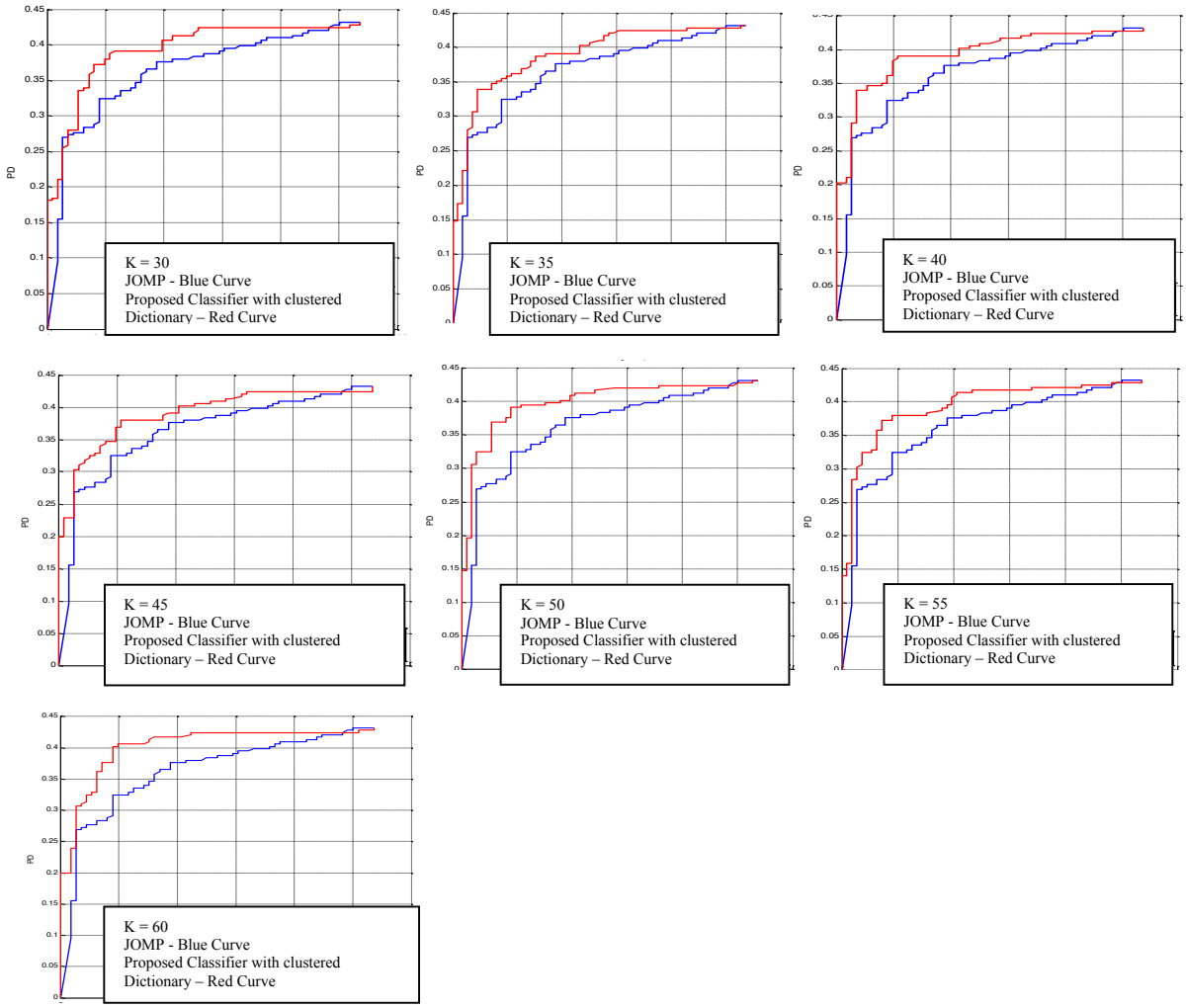

Figure 11: ROC comparisons between JOMP and proposed classifier using clustered dictionary (K=30, 35, 40 …,60), All ROC curves have the same x-axis scale for comparison.

4.5. Model-based Dictionary Estimation

In order to tailor the dictionary to the training data, the training data was divided by class type. These dictionary elements were then used with the proposed classifier to find the frequency of the element picked by each target. The classifier results when compared to JOMP pre-screener are as shown,

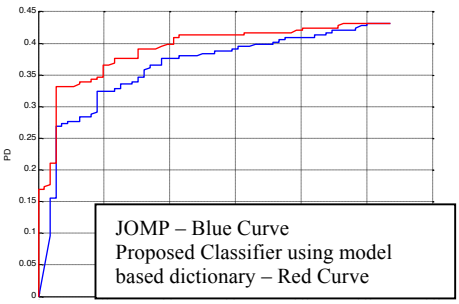

Figure 12: ROC showing the comparison of JOMP pre-screener to the proposed classifier using dictionary estimated using model based method.

The classifier results are improved when compared to the JOMP pre-screener. However, this dictionary does not out-perform the parametric DSRF dictionary. However, the results being similar, this approach can provide the added advantage in terms of computational speed since now for each test point the MP computations can be reduced as many fewer dictionary elements are used.

4.6. Summary and Future work

The classifier presented in this paper is able to discriminate between the different mine types in WEMI data using a possibilistic K-NN classifier. Results are shown on a WEMI data set with 17 classes including a clutter class. The results show that, in 10-fold cross-validation, a classification accuracy of 64% across the 17 classes was achieved using the DSRF dictionary. Also, for mine versus non-mine results were obtained using three different dictionaries. The DSRF dictionary resulted with some-what better performance in the mine versus non-mine results. However, the estimated dictionary results were comparable with a significantly fewer number of dictionary elements. Future work will include the investigation of training ordered weighted average, OWA, operators to combine the individual class confidences to determine an overall mine versus non-mine confidence. Also, as the choice of the dictionary plays an important role in the performance of this classifier, further investigation into dictionary estimation will be conducted.

ACKNOWLEDGEMENTS

This work was supported in part by the Army Research Office. The views and conclusions contained in this document are those of the authors and should not be interpreted as representing the official policies either expressed or implied, of the Army Research Office, Army Research Laboratory, or the U.S. Government. The U.S. Government is authorized to reproduce and distribute reprints for Government purposes notwithstanding any copyright notation hereon.

REFERENCES

[1] W. Scott, “Broadband array of Electromagnetic Induction Sensors for Detecting Buried Landmines” in Proc, IGARSS, pages: 375-378, Jul. 2008

[2] P. Gao, L. Collins, P. Garber, N. Geng, and L. Carin, “Classification of Landmine-Like Metal Targets Using Wideband Electromagnetic Induction,” IEEE Transactions on Geoscience and Remote Sensing, Vol. 38, No. 3, May 2000.

[3] L. Collins, P. Gao, and L. Carin, “An Improved Bayesian Decision Theoretic Approach for Land Mine Detection,” IEEE Transactions on Geoscience and Remote Sensing, Vol. 37, No. 2, March 1999.

[4] L. Collins, P. Gao, L. Makowsky, J. Moulton, D. Reidy and D. Weaver, “Improving detection of low-metallic content landmines using EMI data” IEEE transactions, Geoscience and Remote Sensing Symposium, 2000. IGARSS, vol.4, pages 1631 - 1633

[5] P. Gao, L. Collins, N. Geng and L. Carin “Classification of buried metal objects using wideband frequency-domain electromagnetic induction responses: a comparison of optimal and sub-optimal processors” IEEE Transactions, Geoscience and Remote Sensing Symposium, IGARSS Proceedings. International, vol. 3, pages: 1819 – 1822

[6] H. Frigui, L. Zhan and P. Gader,” Context-Dependent Multi-Sensor Fusion For Landmine Detection” Geoscience and Remote Sensing Symposium, 2008. IGARSS 2008. vol. 2, pages: 371-374

[7] S. Yuksel, G. Ramachandran, P. Gader, J. Wilson, K. Ho and G. He,” Hierarchical Methods For Landmine Detection With Wideband Electro-Magnetic Induction And Ground Penetrating Radar Multi-sensor Systems” Geoscience and Remote Sensing Symposium, 2008. IGARSS 2008. IEEE International, vol. 2, pages 177-18, July 2008

[8] Y. Pati, R. Rezaiifar, and P. Krishnaprasad, “Orthogonal matching pursuit: Recursive function approximation with applications to wavelet decomposition," Signals, Systems and Computers, vol. 1, pages: 40-44, Nov 1993.

[9] G. Ramachandran, P. Gader, and J. Wilson, “GRANMA: Gradient Angle Model Algorithm on Wideband EMI Data for Land-Mine Detection,” IEEE Geosci. and Remote Sens., Vol. 7, No. 3, July 2010

[10] E. Fails, P. Torrione, W. Scott, and L. Collins, “Performance of a four parameter model for landmine signatures in frequency domain wideband electromagnetic induction detection systems,” in Proceedings of the SPIE: 2007 Annual International Symposium on Aerospace/Defense Sensing, Simulation, and Controls, Vol. 6553, May 2007

[11] S. A. Dudani, "The distance weighted k-nearest neighbor rule" IEEE Trans, Syst., Man, Cybern., vol. SMC-6, no. 4, pages: 325-327, Apr. 1976
[12] J. M. Keller, M. R. Gray, and J. A. Givens, "A fuzzy k-nearest neighbor algorithm" IEEE Trans. Syst., Man, Cybern., vol. SMC-15, no. 4, pages: 580–585, Jul./Aug. 1985
[13] H. Frigui and P. Gader, "Detection and Discrimination of Land Mines in Ground-Penetrating Radar Based on Edge Histogram Descriptors and a Possibilistic K-Nearest Neighbor Classifier" IEEE Trans. Fuzzy Systems, Vol. 17, No. 1, Feb. 2009
[14] M. Wei, W. Scott and J. McClellan, "Robust Estimation of the Discrete Spectrum of Relaxations for Electromagnetic Induction Responses" IEEE Trans. Geosci. Remote Sens, Vol. 48, No. 3, March 2010
[15] S. Goldberg, T. Glenn, J. Wilson, P. Gader, "Landmine Detection using Two- tapped Joint Orthogonal Matching Pursuits," Proceedings of the SPIE, vol. 8357, Detection and Sensing of Mines, Explosive Objects, and Obscured Targets XVII, April 2012.